

A two-loop contribution to $B_s \rightarrow \mu^+ \mu^-$ at large $\tan \beta$ in the MSSM

Seungwon Baek¹

KIAS, 207-43 Cheongryangni 2-dong, Seoul 130-722, Korea

Abstract

We consider a two-loop contribution of Higgs-mediated penguin diagram to $B_s \rightarrow \mu^+ \mu^-$ at large $\tan \beta$ in the MSSM, motivated by a recently proposed two-loop magnetic penguin diagrams by Chen and Geng [1]. Typically the two-loop diagram is a μ_s correction to the one-loop contributions. However the new contribution can dominate one-loop contributions in a region of parameter space where μ_s , A_t and A_b are very large and scalar top, scalar bottom and charged Higgs are light. Both constructive and destructive interferences are possible. The total branching ratio can be drastically changed from the one-loop result.

April 2004

¹email: swbaek@kias.re.kr

1 Introduction

In the minimal supersymmetric standard model (MSSM) the large $\tan\beta$ scenario is getting more and more interesting because the small $\tan\beta$ region ($\tan\beta < 3$) is already disfavored from the Higgs particle search [2] and the top and bottom Yukawa coupling constants can be unified at GUT scale if $\tan\beta$ is large ($\tan\beta \sim 50$). If $\tan\beta$ is large, the phenomenology of MSSM can be quite different from the small $\tan\beta$ case.

At the tree-level up-type (down-type) Higgs field couples only to up-type (down-type) quark fields, and there is no Higgs-mediated flavor changing neutral current (FCNC) by holomorphy of superpotential. However, the soft supersymmetry breaking terms induce effective Lagrangian which couples Higgs fields to different types of quark fields. As a consequence, at large $\tan\beta$, Higgs-mediated FCNCs are generated [3] as well as the large corrections to the down-type Yukawa couplings [4] and CKM matrix elements [5].

This Higgs-mediated FCNC effects are most conspicuous in the rare processes like $B_s \rightarrow \mu^+ \mu^-$ decay [3] and $B_s^0 \rightarrow \bar{B}_s^0$ mixing [6]. Especially the branching ratio of $B_s \rightarrow \mu^+ \mu^-$ decay is proportional to the $\tan^6\beta$ and can be enhanced by several order of magnitude over the standard model (SM) expectation, allowing this mode to be produced at current colliders such as Tevatron. The current experimental bound is [7]

$$B(B_s \rightarrow \mu^+ \mu^-) < 5.8 \times 10^{-7} \quad (1)$$

at 90% confidence level.

In this paper we consider a Higgs-mediated two-loop FCNC diagram shown in Fig. 1 motivated by a recent finding by Chen and Geng [1]. They showed that two-loop magnetic penguin diagrams with Higgs field replaced by photon (or gluon) can give significant deviation in the CP asymmetry of $B \rightarrow K_s$ in the CP violating MSSM [1].

We show that the two-loop contribution to $B_s \rightarrow \mu^+ \mu^-$, although suppressed by α_s compared to the one-loop, can compete or even dominate the one-loop contribution in some region of MSSM parameter space. As a result, the total branching ratio can be drastically different from the one-loop calculation. We consider the CP conserving scenario in this paper because the CP violating phases in the MSSM parameters are very strongly

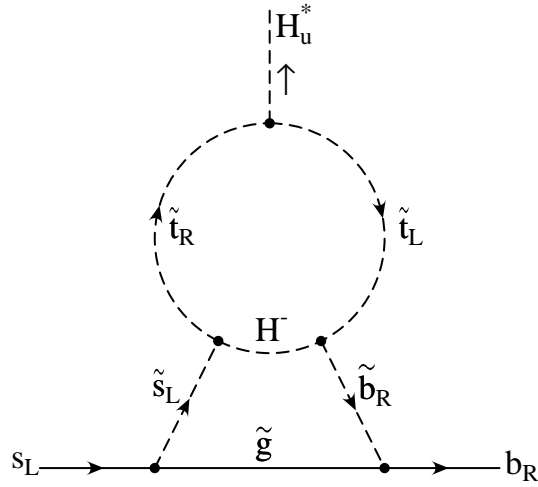


Figure 1: Two-loop contributions to the Higgs-mediated $b_R \rightarrow s_L$ transition.

constrained at large $\tan \beta$ due to the two-loop Barr-Zee type diagram [3].

This paper is organized as follows. In Section 2 we outline our approach to calculate the two-loop contribution to $B_s \rightarrow \mu^+ \mu^-$ and present its analytic formula. Numerical analyses are done in Section 3. Conclusions are contained in Section 4.

2 A two-loop contribution to $B_s \rightarrow \mu^+ \mu^-$ decay at large $\tan \beta$

To calculate the decay amplitude for the $B_s \rightarrow \mu^+ \mu^-$ decay we work in the effective Lagrangian approach [3, 6]. As mentioned in the Introduction, at tree level, diagonalizing the Yukawa matrices automatically guarantees the absence of the Higgs-mediated FCNCs. In this basis we have

$$\mathcal{L}_e = \overline{u}_R \hat{Y}_u Q_L + \overline{d}_R \hat{Y}_d Q_L + H_u + \text{h.c.}; \quad (2)$$

where $A = B = {}^{ij}A_i B_j = A_1 B_2 - A_2 B_1$, $Q = (V^Y u_L; d_L)^T$ with CKM matrix V , and \hat{Y}_u and \hat{Y}_d are diagonal Yukawa matrices. All the loop calculations are done in this "super-CKM" (SCKM) basis. We also assume that the scalar quark mass matrices are also flavor diagonal

in the SCKM basis. Therefore the only source of FCNC is the off-diagonal CKM matrix elements.

The soft supersymmetry breaking terms generate the "nonholomorphic" terms at one-loop level. These corrections make the effective Lagrangian for the down-type quarks become in the form [3, 6]

$$L_e = \overline{d_R} (\hat{Y}_d + \delta Y_d) Q + H_d + H_u \overline{d_R} + u Y_d Q : \quad (3)$$

The one-loop diagrams which contribute to δY_d are shown in Fig. 2. The diagram shown in Fig. 2 (b) is proportional to the up-type Yukawa matrix. Consequently the two terms in the effective Lagrangian (3) cannot be diagonalized simultaneously in the flavor space, necessarily generating Higgs-mediated FCNCs. We do not include the term δY_d in the analysis because it is not enhanced by $\tan \beta$ and therefore plays subdominant role in $B_s \rightarrow K^0$ decay.

The corrections δY_d are given in the form [6]

$$(\delta Y_d)_{ij} = Y_{d_i} \delta_{ij} + Y_t Y_t^2 V_{3i} V_{3j} ; \quad (4)$$

where V_{ij} are CKM matrix elements. Here δ_{ij} does not change the flavor if the down-type scalar mass matrix does not have flavor changing off-diagonal terms. However Y_t is flavor changing through the CKM matrix elements even if there are no flavor off-diagonal elements in the up-type squark mass matrix. The one-loop results are given by

$$\begin{aligned} \delta_{ij} &= \frac{2}{3} \frac{g_s}{m_g} j(y_{\mathcal{Q}_{1g}}; y_{\mathcal{Q}_{1g}}) - \frac{2}{3} \frac{g_s}{m_g} \frac{\sin^2 2\beta}{4} j(y_{\mathcal{B}_{1g}}; y_{\mathcal{B}_{1g}}); \\ \delta_{ij}^{(1)} &= \frac{1}{16} \frac{A_t}{m_t^2} j(y_{\mathcal{Q}_{3g}}; y_{\mathcal{Q}_{3g}}) - \frac{1}{16} \frac{A_t}{m_t^2} \frac{\sin^2 2\alpha}{4} j(y_{\mathcal{E}_{1g}}; y_{\mathcal{E}_{1g}}); \end{aligned} \quad (5)$$

where $y_{\mathcal{Q}_{1g}} = m_{\mathcal{Q}_{1g}}^2/m_g^2$, etc., $\mathcal{B}_{1g}; \mathcal{E}_{1g}$ are lighter mass eigenstates, β, α are mixing angles of the mass matrices, and the loop function $j(x; y)$ is defined as

$$j(x; y) = \frac{j(x) - j(y)}{x - y}; \quad \text{for } j(x) = \frac{x \log x}{x - 1} : \quad (6)$$

The superscript (1) in $\delta_{ij}^{(1)}$ denotes one-loop contribution.

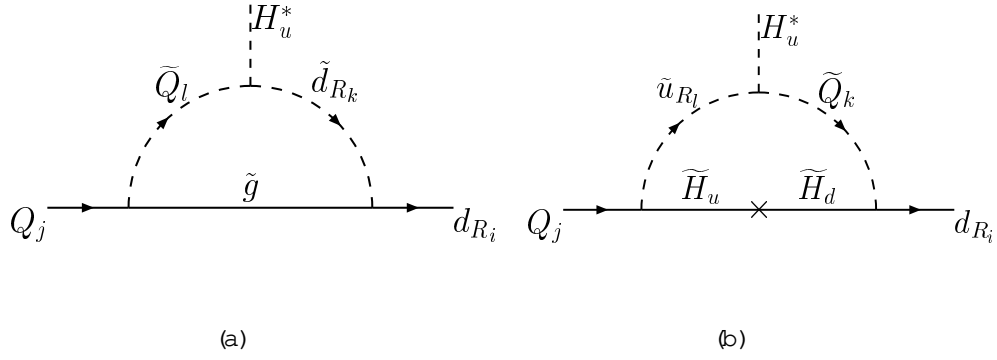


Figure 2: One-loop contributions to the corrections δY_d .

The two-loop diagram in Fig. 1 contributions to the FCNC parameter δY is found to be

$$\delta Y^{(2)} = \frac{g_s^2}{24} \frac{A_t A_b}{m_g^3} \frac{\sin^2 2\theta_t \sin^2 \theta_b \sin^2 \theta_s}{4} J \frac{m_{e_1}^2}{m_g^2} i \frac{m_{e_1}^2}{m_g^2} i \frac{m_{e_1}^2}{m_g^2} i \frac{m_H^2}{m_g^2} \quad (7)$$

where $\theta_{t(b;s)}$ is mixing angle in the scalar top (bottom, strange) mass matrix and

$$J = \frac{m_{e_1}^2}{m_g^2} i \frac{m_{e_1}^2}{m_g^2} i \frac{m_{e_1}^2}{m_g^2} i \frac{m_H^2}{m_g^2} \\ = \int_0^1 dx \int_0^1 dQ^2 \frac{m_g^4 (1-x)Q^2}{(Q^2 + m_g^2)(Q^2 + m_{e_1}^2)(Q^2 + m_{e_1}^2)(1-x)m_{e_1}^2 + xm_H^2 + x(1-x)Q^2} \quad (8)$$

We included only the contributions of lighter squarks.

In the operator basis given in ref. [6], the Wilson coefficients for the Higgs-mediated penguin operators are approximated at large $\tan \beta$ to be

$$C_S \approx C_P \approx \frac{m_{\bar{t}}^2}{4m_W^2 m_A^2} \frac{16 Y \tan^3 \beta}{(1 + e_3 \tan \beta)(1 + e_0 \tan \beta)} \quad (9)$$

where $Y = Y^{(1)} + Y^{(2)}$ and $e_3 = e_0 + Y_{t^2}^2$. Note that C_S and C_P are proportional to $\tan^3 \beta$, which makes possible the large enhancement of $B(B_s \rightarrow \mu^+ \mu^-)$ at large $\tan \beta$. The contribution of chirality-flipped operators with respect to Q_S and Q_P are suppressed by $m_s = m_b$. In an excellent approximation we have [6]

$$B(B_s \rightarrow \mu^+ \mu^-) = 2.32 \cdot 10^{-6} \frac{B_s}{1.5\text{ps}} \left(\frac{F_{B_s}}{230\text{MeV}} \right)^2 \left(\frac{Y_{ts}^e}{0.040} \right)^2$$

$$\mathcal{C}_S^j + \mathcal{C}_P^i + 0.04 C_A^j \quad (10)$$

where $\mathcal{C}_S = m_{B_s} C_S$ and $\mathcal{C}_P = m_{B_s} C_P$. The contribution of Wilson coefficient C_A to the branching ratio has a suppression factor $2m_{B_s} = 0.04$ in front of it and we fix C_A by its SM value $C_A = 0.97$ for simplicity.

Now several comments are in order: 1) From the analytic formula (7) it is clear that large two-loop contributions are possible if μ , A_t , and A_b are large and $m_{\tilde{e}_1}$, $m_{\tilde{e}_1(\tilde{e}_1)}$, and m_H are small. We should mention that these parameters do not occur naturally in the usually considered supersymmetric models, such as, gravity-mediated, gauge-mediated models etc. However they are phenomenologically acceptable [2] and should be tested experimentally. 2) The corresponding two-loop diagrams with charged Higgs inside the loop considered in [9] can also generate FCNC. However it is suppressed by electroweak gauge coupling constants. 3) There are other diagrams with similar topology with Fig. 1. Since they do not generate FCNC, we do not include them in this work.

3 Numerical Results

The large values of μ (or A_t) can generate too large values in the off-diagonal components in the scalar quark mass matrices, breaking the color or electric charges. To avoid these dangerous situation while allowing large values of μ (or A_t) we follow the approach considered in [9]. We take the lighter mass eigenvalues of squarks, $m_{\tilde{e}_1}$ or $m_{\tilde{e}_1}$ as inputs instead of soft mass parameters $m_{\tilde{Q}_3}$, $m_{\tilde{e}_R}$ or $m_{\tilde{e}_R}$. We also assume the maximal mixing of scalar quarks ($\mu_t = \mu_b = 4$) and $m_{\tilde{e}_1} = m_{\tilde{e}_1}$ to maximize the two-loop contributions.

In Fig. 3 we show the ratio $\mathcal{B}^{(2)} = \mathcal{B}^{(1)}$ as a function of μ . Other parameters are taken to be $m_{\tilde{e}_1} = m_{\tilde{e}_1} = 100$ GeV, $m_H = 200$ GeV, $A_b = 2$ TeV and $m_{\tilde{g}} = 300; 500; 700$ GeV. The ratio is independent of $\tan\beta$ and A_t . We can see that the two-loop contributions can easily dominate one-loop contributions as μ increases. The relative sign between $\mathcal{B}^{(2)}$ and $\mathcal{B}^{(1)}$ can be flipped by changing the sign of either $m_{\tilde{g}}$ or A_b .

In Fig. 4 we show plots of $\mathcal{B}(\mathcal{B}_s \rightarrow \mu^+ \mu^-)$ as a function of μ . We take $m_{\tilde{e}_1} = m_{\tilde{e}_1} = 100$ GeV, $m_{\tilde{g}} = 300$ GeV, $m_H = 200$ GeV, $A_t = 2$ TeV and $A_b = +2(-2)$ TeV for Fig. 4 (a)

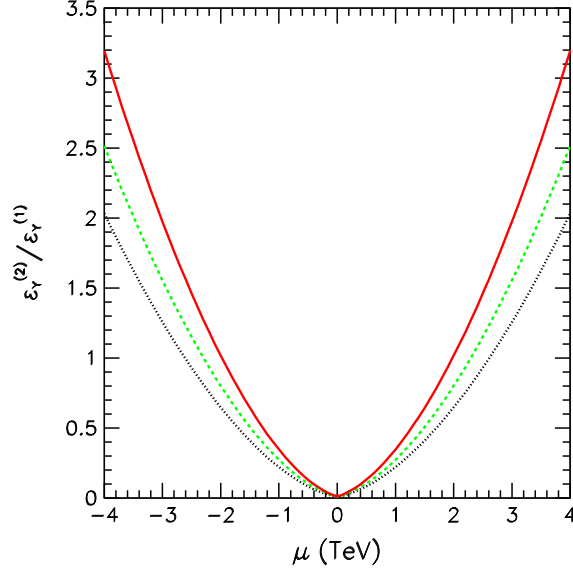


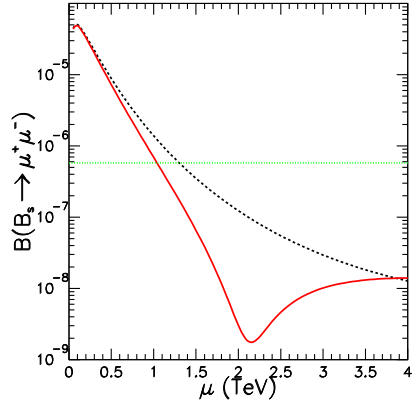
Figure 3: $\epsilon_Y^{(2)}/\epsilon_Y^{(1)}$ as a function of μ for $m_{\tilde{e}_1} = m_{\tilde{\nu}_1} = 100 \text{ GeV}$, $m_H = 200 \text{ GeV}$, $A_b = 2 \text{ TeV}$ and $m_g = 300; 500; 700 \text{ GeV}$ (from above).

(for Fig. 4 (b)). We can see strong destructive (constructive) interference depending on the sign of A_b . Especially in Fig. 4 (a), the two-loop contribution almost exactly cancels the one-loop contribution near $\mu = 2:1 \text{ TeV}$, resulting in a dip in the plot.

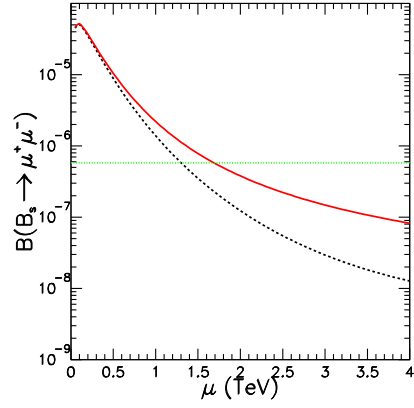
Fig. 5 shows $B(B_s \rightarrow \mu^+ \mu^-)$ as a function of A_t . For these plots we take $\mu = 2 \text{ TeV}$, $m_g = 500 \text{ GeV}$, and other parameters the same as in Fig. 4. We can see large values of A_t can change the $B(B_s \rightarrow \mu^+ \mu^-)$ by an order of magnitude.

In Fig. 6 plots of $B(B_s \rightarrow \mu^+ \mu^-)$ as a function of $m_{\tilde{e}_1}$ are shown. For these plots we take $\mu = 2 \text{ TeV}$, and other parameters the same as in Fig. 4. They show the effects of two-loop diagrams are significant for small values of $m_{\tilde{e}_1}$.

In Fig. 6 plots of $B(B_s \rightarrow \mu^+ \mu^-)$ as a function of $m_{\tilde{\nu}_1}$ are given. For these plots we take $\mu = 4 \text{ TeV}$, $m_g = 0:5 \text{ TeV}$, and other parameters the same as in Fig. 4. We can see the two-loop effect rapidly decouples as $m_{\tilde{\nu}_1}$ increases. At one-loop level, $m_{\tilde{\nu}_1}$ appears only in ϵ_0 as can be seen in (5), which suppresses (9) for light $\tilde{\nu}_1$ for $\epsilon_0 > 0$. As $\tilde{\nu}_1$ becomes heavier, ϵ_0 decreases and (9) also increases. This is the reason why the $B(B_s \rightarrow \mu^+ \mu^-)$'s increase

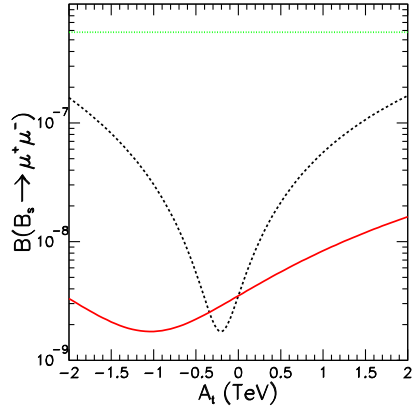


(a)

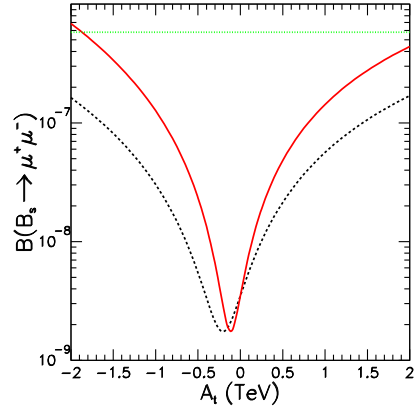


(b)

Figure 4: $B(B_s \rightarrow \mu^+ \mu^-)$ as a function of μ . We take $\tan \beta = 60, m_{\tilde{e}_L} = m_{\tilde{e}_R} = 100 \text{ GeV}, m_{\tilde{g}} = 300 \text{ GeV}, m_H = 200 \text{ GeV}, A_t = 2 \text{ TeV}$, (a) $A_b = 2 \text{ TeV}$ and (b) $A_b = -2 \text{ TeV}$. The (black) dashed line represents one-loop contribution, (red) solid line represents total contribution. The horizontal line is the current experimental bound.

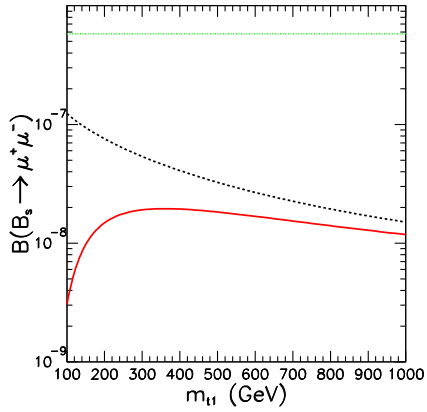


(a)

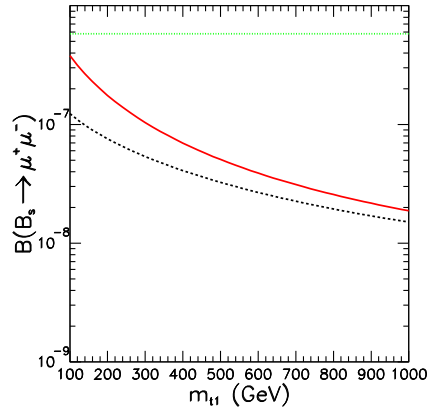


(b)

Figure 5: $B(B_s \rightarrow \mu^+ \mu^-)$ as a function of A_t . We take $\mu = 2 \text{ TeV}, m_{\tilde{g}} = 0.5 \text{ TeV}$, (a) $A_b = 2 \text{ TeV}$ and (b) $A_b = -2 \text{ TeV}$. Others are the same as Fig. 4.

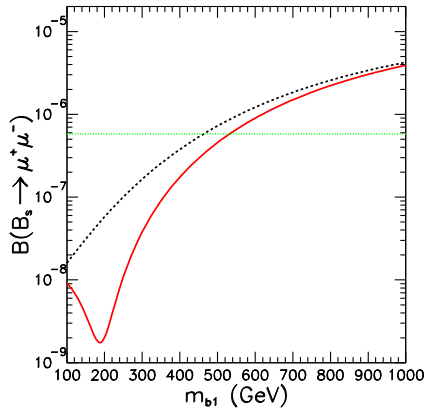


(a)

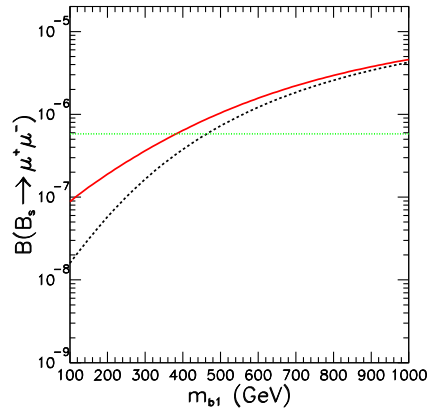


(b)

Figure 6: $B(B_s \rightarrow \mu^+ \mu^-)$ as a function of $m_{\tilde{t}_1}$. We take $\mu = 2 \text{ TeV}$, (a) $A_b = 2 \text{ TeV}$ and (b) $A_b = 1 \text{ TeV}$. Others are the same as Fig. 4.



(a)



(b)

Figure 7: $B(B_s \rightarrow \mu^+ \mu^-)$ as a function of $m_{\tilde{b}_1}$. We take $\mu = 4 \text{ TeV}$, $m_g = 0.5 \text{ TeV}$, (a) $A_b = 2 \text{ TeV}$ and (b) $A_b = 1 \text{ TeV}$. Others are the same as Fig. 4.

as $m_{\tilde{b}_1}$ increases before they saturate for very heavy \tilde{b}_1 .

We have also checked the dependence of $B(B_s \rightarrow \mu^+ \mu^-)$ on gluino mass. It turns out

the branching ratio decreases rather slowly as m_g increases.

4 Conclusions

We studied a Higgs-mediated two-loop diagram which can significantly change the one-loop contribution to the rare decay $B \rightarrow B_s \mu^+ \mu^-$ at large $\tan \beta$ in the MSSM. This two-loop diagram, although suppressed by α_s , can compete with or even dominate the one-loop diagram contributions for large values of μ , A_t and A_b and for small values of $m_{\tilde{e}_1}$, $m_{\tilde{e}_2}$ and m_H . It has mild dependence on the gluino mass parameter. Depending on the sign of the parameters both constructive and destructive interferences are possible. For the constructive interference, the experimental bound on the $B \rightarrow B_s \mu^+ \mu^-$ more strongly constrains the MSSM parameters. For the destructive interference, it is a possibility that we may not see the event even though one-loop result predicts large branching ratios.

Acknowledgment

The author is grateful to Francesca Borzumati for useful discussions.

References

- [1] C. H. Chen and C. Q. Feng, [arXiv:hep-ph/0403188](#).
- [2] K. Hagiwara et al. [Particle Data Group Collaboration], *Phys. Rev. D* **66**, 010001 (2002).
- [3] S. R. Choudhury and N. Gaur, *Phys. Lett. B* **451**, 86 (1999) [[arXiv:hep-ph/9810307](#)]; K. S. Babu and C. F.olda, *Phys. Rev. Lett.* **84**, 228 (2000) [[arXiv:hep-ph/9909476](#)]; C. S. Huang, W. Liao, Q. S. Yan and S. H. Zhu, *Phys. Rev. D* **63**, 114021 (2001) [Erratum -*ibid.* **D 64**, 059902 (2001)] [[arXiv:hep-ph/0006250](#)]; P. H. Chankowski and L. Slawianowska, *Phys. Rev. D* **63**, 054012 (2001) [[arXiv:hep-ph/0008046](#)]; G. Isidori and A. Retico, *JHEP* **0111**, 001 (2001) [[arXiv:hep-ph/0110121](#)]; *JHEP* **0209**, 063

(2002) [[arXiv:hep-ph/0208159](#)]; C. Bobeth, T. Ewerth, F. Krüger and J. Urban, Phys. Rev. D 64, 074014 (2001) [[arXiv:hep-ph/0104284](#)]; Phys. Rev. D 66, 074021 (2002) [[arXiv:hep-ph/0204225](#)]; A. Dedes, H. K. Dreiner and U. Nierste, Phys. Rev. Lett. 87, 251804 (2001) [[arXiv:hep-ph/0108037](#)]; C. Bobeth, A. J. Buras, F. Krüger and J. Urban, Nucl. Phys. B 630, 87 (2002) [[arXiv:hep-ph/0112305](#)]; R. Aomawa, B. Dutta, T. Kamon and M. Tanaka, Phys. Lett. B 538, 121 (2002) [[arXiv:hep-ph/0203069](#)]; S. Baek, P. Ko and W. Y. Song, Phys. Rev. Lett. 89, 271801 (2002) [[arXiv:hep-ph/0205259](#)]; JHEP 0303, 054 (2003) [[arXiv:hep-ph/0208112](#)]; A. Dedes, H. K. Dreiner, U. Nierste and P. Richardson, [arXiv:hep-ph/0207026](#); G. D'Ambrosio, G. F. Giudice, G. Isidori and A. Strumia, Nucl. Phys. B 645, 155 (2002) [[arXiv:hep-ph/0207036](#)]; J. K. Mizukoshi, X. Tata and Y. Wang, Phys. Rev. D 66, 115003 (2002) [[arXiv:hep-ph/0208078](#)]; T. Ibrahim and P. Nath, Phys. Rev. D 67, 016005 (2003) [[arXiv:hep-ph/0208142](#)]; A. Dedes and A. Pilaftsis, Phys. Rev. D 67, 015012 (2003) [[arXiv:hep-ph/0209306](#)]; C. S. Huang and X. H. Wu, Nucl. Phys. B 657, 304 (2003) [[arXiv:hep-ph/0212220](#)]; R. Demisek, S. Raby, L. Roszkowski and R. Ruiz De Austri, JHEP 0304, 037 (2003) [[arXiv:hep-ph/0304101](#)]; T. Blazek, S. F. King and J. K. Parry, [arXiv:hep-ph/0308068](#); G. L. Kane, C. Kolda and J. E. Lennon, [arXiv:hep-ph/0310042](#).

[4] L. J. Hall, R. Rattazzi and U. Sarid, Phys. Rev. D 50, 7048 (1994) [[arXiv:hep-ph/9306309](#)].

[5] T. Blazek, S. Raby and S. Pokorski, Phys. Rev. D 52, 4151 (1995) [[arXiv:hep-ph/9504364](#)];

[6] A. J. Buras, P. H. Chankowski, J. Rosiek and L. Slawianowska, Nucl. Phys. B 659, 3 (2003) [[arXiv:hep-ph/0210145](#)].

[7] D. A. Costa et al. [CDF Collaboration], [arXiv:hep-ex/0403032](#).

[8] D. Chang, W. Y. Keung and A. Pilaftsis, Phys. Rev. Lett. 82, 900 (1999) [Erratum – *ibid.* 83, 3972 (1999)] [[arXiv:hep-ph/9811202](#)].

- [9] C . H . Chen and C . Q . G eng, Phys. Lett. B 511, 77 (2001) [[arX iv:hep-ph/0104151](#)];
A . A rhib and S . B aek, Phys. Rev. D 65, 075002 (2002) [[arX iv:hep-ph/0104225](#)].